Luminescent Characterization of Solution Oligomerization Process Mediated Gold−Gold Interactions. DFT Calculations on [Au₂Ag₂R₄L₂]ₙ Moieties

Eduardo J. Fernández,[‡] M. Concepción Gimeno,[§] Antonio Laguna,[*,§]
José M. López-de-Luzuriaga,[‡] Miguel Monge,[‡,⊥] Pekka Pyykkö,[*,⊥] and Dage Sundholm[⊥]

Contribution from the Departamento de Química, Universidad de la Rioja, Grupo de Síntesis
Química de La Rioja, UA-CSIC, Obispo Bustamante 3, 26001 Logroño, Spain, Departamento de
Química Inorgánica, Instituto de Ciencia de Materiales de Aragón, Universidad de Zaragoza-CSIC,
50009 Zaragoza, Spain, and Department of Chemistry, University of Helsinki, P.O.B. 55
(A. I. Virtasen aukio 1), FIN-00014 Helsinki, Finland

Abstract: The optical properties of [Au₂Ag₂(C₆F₅)₄(OCMe₂)₂]ₙ (**1**) have been studied in the solid state at room temperature and at 77 K and in acetone solution (5×10^{-4} M). The crystal structure of **1**, analyzed by X-ray diffraction, consists of polymeric chains formed by repetition of Au₂Ag₂ moieties linked through short gold−gold interactions. The emission profile observed for **1** in dilute acetone solution (5×10^{-4} M) is assignable to pentafluorophenyl localized $\pi\pi^*$ excited states or from π-MMCT transitions, and in the solid-state arises from metal-centered $(d\sigma^*)^1(p\sigma)^1$ or $(d\delta^*)^1(p\sigma)^1$ excited states. When the absorption and emission spectra of compound **1** in acetone are registered at different concentrations, they display a band that does not obey the Lambert−Beer law. This deviation is consistent with molecular aggregation in solution through gold−gold interactions, and a clear correlation between the emission wavelength and the structure of **1** in the solid state and in solution is shown. DFT calculations accord with the observed experimental behavior and show the nature of the orbitals involved in each transition.

Introduction

As has been well established, closed shell d¹⁰ atoms such as gold(I) have a marked tendency to form dimers, oligomers, and polymers, a fact of interest to both theoretical and experimental chemists.[1−8] Particularly interesting are extended linear chain

* Address correspondence to these authors. A.L.: E-mail alaguna@ posta.unizar.es. P.P.: E-mail pekka.pyykko@helsinki.fi.
‡ Universidad de la Rioja, UA-CSIC.
§ Universidad de Zaragoza-CSIC.
⊥ University of Helsinki.

(1) (a) Pyykkö, P. *Chem. Rev.* **1997**, *97*, 597. (b) Pyykkö, P.; Zhao, Y. *Angew. Chem., Int. Ed. Engl.* **1995**, *34*, 1894. (c) Pyykkö, P.; Li, J.; Runeberg, N. *Chem. Phys. Lett.* **1994**, *218*, 133. (d) Pyykkö, P.; Zhao, Y. *Chem. Phys. Lett.* **1991**, *177*, 103. (e) Rösch, N.; Görling, D. E.; Schmidbaur, H. *Angew. Chem., Int. Ed. Engl.* **1989**, *28*, 1357.(f) Burdett, J. K.; Eisenstein, O.; Schweizer, W. B. *Inorg. Chem.* **1994**, *33*, 3261.
(2) (a) Schmidbaur, H. *Chem. Soc. Rev.* **1995**, 391. (b) Schmidbaur, H. *Interdiscip. Sci. Rev.* **1992**, *17*, 213. (c) Schmidbaur, H. *Gold Bull.* **1990**, *23*, 211.
(3) (a) Vickery, J. C.; Balch, A. L. *Inorg. Chem.* **1997**, *36*, 5978. (b) Calcar, P. M. V.; Olmstead, M. M.; Balch, A. L. *J. Chem. Soc., Chem. Commun.* **1995**, 1773.
(4) (a) Puddephatt, R. J. *Chem. Commun.* **1998**, 1055. (b) *The Chemistry of Gold*; Elsevier: Amsterdam, 1978.
(5) (a) Fernández, E. J.; López-de-Luzuriaga, J. M.; Monge, M.; Rodríguez, M. A.; Crespo, O.; Gimeno, M. C.; Laguna, A.; Jones, P. G. *Inorg. Chem.* **1998**, *37*, 6002. (b) Gimeno, M. C.; Laguna, A. *Chem. Rev.* **1997**, *97*, 511.
(6) (a) Mingos, D. M. P.; Yau, J.; Menzer, S.; Williams, D. J. *Angew. Chem., Int. Ed. Engl.* **1995**, *34*, 1894, (b) Mingos, D. M. P. *J. Chem. Soc., Dalton Trans.* **1996**, 561.
(7) (a) Shieh, S.-J.; Hong, X.; Peng, S.-M.; Che, C.-M. *J. Chem. Soc., Dalton Trans.* **1994**, 3067. (b) Tzeng, B.-C.; Cheung, K.-K.; Che, C.-M. *Chem. Commun.* **1996**, 1681. (c) Tzeng, B.-C.; Che, C.-M.; Peng, S.-M. *Chem Commun.* **1997**, 1771.

compounds, because the rationalization of the bonding in these structures still remains a challenge and because the linear chain complexes have spectacular potential as possible sensors for volatile organics as described by Mann for [PtL₄][M(CN)₄] (L = arylisonitrile; M = Pt, Pd)[9] and Eisenberg for [Au(S₂-CN(C₅H₁₁)₂)]₂[10] in many cases showing intense emissions in the solid state.

In particular it seems established that the presence of gold-(I)−gold(I) interactions is critical to the optical properties when the gold atoms are in a linear environment.[11] Thus, Fackler et al.[12] have analyzed the metal−metal interactions in dinuclear gold(I) compounds and have shown that the metal-centered luminescence of gold dimers in the solid state and in solution is due to either $(d\sigma^*)^1(p\sigma)^1$ or $(d\delta^*)^1(p\sigma)^1$ excited states. In some cases discrete dimers such as [Au₂(P−P)₂]²⁺ (P−P = bis-(diphenylphosphino)methane) are emissive in the solid state and in solution,[12−15] while in the case of [Au(S₂CN(C₅H₁₁)₂)]₂ the colorless discrete-molecular form is nonemissive and the orange

(8) (a) Davila, R. M.; Elduque, A.; Grant, T.; Staples, R. J.; Fackler, J. P., Jr. *Inorg. Chem.* **1993**, *32*, 1749. (b) Davila, R. M.; Staples, R. J.; Elduque, A.; Harlass, M.; Kyle, L.; Fackler, J. P., Jr. *Inorg. Chem.* **1994**, *33*, 5940.
(9) Exstrom, C. L.; Sowa, J. R., Jr.; Daws, C. A.; Janzen, D.; Mann, K. R. *Chem. Matter.* **1995**, *7*, 15.
(10) Mansour, M. A.; Connick, W. B.; Lachicotte, R. J.; Gysling, H. J.; Eisenberg, R. *J. Am. Chem. Soc.* **1998**, *120*, 1329.
(11) Forward, J. M.; Fackler, J. P., Jr.; Assefa, Z. Photochemical Properties of Gold(I) Complexes. In *Optoelectronic Properties of Inorganic Compounds*; Roundhill, D. M., Fackler, J. P., Jr., Eds.; Plenum Press: New York, 1999; pp 195−226.
(12) King, C.; Wang, J.-C.; Khan, M. N. I.; Fackler, J. P., Jr. *Inorg. Chem.* **1989**, *28*, 2145.

form, composed of discrete dimers stacked along the *c* axis to form an infinite chain of Au atoms with short intermolecular contacts, exhibits intense luminescence.[10] In addition, a very recent study by Fackler[16] has shown a strong dependence of the emission spectra on the gold−gold interactions at different temperatures for S−Au−S dinuclear complexes, establishing a correlation between the emission profile and the presence of inter- and/or intramolecular metal−metal interactions in the solid state.

Nevertheless, in most cases, polynuclear d[10] complexes, when dissolved, usually undergo ligand redistribution or else these assemblages tend to dissociate into nonemissive monomeric components.

Although oligomerization processes that would lead to emission of radiation have been observed in solution at high concentrations ($>10^{-3}$ M)[10,17,18] or by comparison of frozen solution (77 K) and solid state for the complex [AuTl(MTP)$_2$] (MTP = [CH$_2$P(S)Ph$_2$]$^-$),[19,20] conclusive evidence has not yet been obtained.

Meanwhile, we have reported the use of the [Au(C$_6$F$_5$)$_2$]$^-$ moiety as a Lewis base in the syntheses of the heterometallic extended linear chain compounds [Au$_2$Ag$_2$(C$_6$F$_5$)$_4$L$_2$]$_n$ (L = neutral ligand)[21] and [Tl(OPPh$_3$)$_2$][Au(C$_6$F$_5$)$_2$].[22] In both cases extended linear chain complexes are formed through gold−gold interactions and gold−thallium interactions in the solid state.

In this paper we report the analogous preparation of an extended linear chain gold−silver complex, along with its crystal structure and a luminescence study in the solid state at room temperature and at 77 K, and also in solution for a wide range of concentrations.

Here we present the first proof based on luminescence studies of an aggregation process of [Au$_2$Ag$_2$(C$_6$F$_5$)$_4$(OCMe$_2$)$_2$] moieties in solution whose behavior can be extrapolated by a simple linear fit to the solid-state data behavior. We have also carried out DFT calculations to assign the molecular orbitals involved in the behavior we observe in solution and in the solid state. In addition, for the first time time-dependent DFT calculations have been used for the prediction of the excitations that lead to emission of radiation in solution and in the solid state.

Experimental Section

General. UV−vis absorption spectra were obtained on a HP 8453 UV−visible spectrophotometer. Excitation and emission spectra were recorded on a Perkin-Elmer LS-50B luminescence spectrometer. Acetone for photophysics was distilled over potassium permanganate and degassed before use.

(13) Che, C.-M.; Kwong, H. L.; Poon, C.-K.; Yam, V. W.-W. *J. Chem. Soc., Dalton Trans.* **1990**, 3215.

(14) Li, D.; Che, C.-M.; Kwong, H. L.; Yam, V. W.-W. *J. Chem. Soc., Dalton Trans.* **1992**, 3325.

(15) Fu, W.-F.; Chan, K.-C.; Miskowski, V. M.; Che, C.-M. *Angew. Chem., Int. Ed. Engl.* **1999**, *38*, 2783.

(16) van Zyl, W. E.; López-de-Luzuriaga, J. M.; Fackler, J. P., Jr. *J. Mol. Struct.* **2000**, *516*, 99.

(17) Lai, S.-W.; Chan, M. C.-W.; Cheung, T.-C.; Peng, S.-M.; Che, C.-M. *Inorg. Chem.* **1999**, *38*, 4046.

(18) (a) Tang, S. S.; Chang, C.-P.; Lin, I. J. B.; Liou, L.-S.; Wang, J.-C. *Inorg. Chem.* **1997**, *36*, 2294. (b) Hao, L.; Lachicotte, R. J.; Gysling, H. J.; Eisenberg, R. *Inorg. Chem.* **1999**, *38*, 4616.

(19) Wang, S.; Fackler, J. P., Jr.; King, C.; Wang, J. C. *J. Am. Chem. Soc.* **1988**, *110*, 3308.

(20) Wang, S.; Garzón, G.; King, C.; Wang, J. C.; Fackler, J. P., Jr. *Inorg. Chem.* **1989**, *28*, 4616.

(21) (a) Usón, R.; Laguna, A.; Laguna, M.; Jones, P. G.; Sheldrick, G. M. *J. Chem. Soc., Chem. Commun.* **1981**, 1097. (b) Usón, R.; Laguna, A.; Laguna, M.; Manzano, B. R.; Jones, P. G.; Sheldrick, G. M. *J. Chem. Soc., Dalton Trans.* **1984**, 285.

(22) Crespo, O.; Fernández, E. J.; Jones, P. G.; Laguna, A.; López-de-Luzuriaga, J. M.; Mendía, A.; Monge, M.; Olmos, E. *Chem. Commun.* **1998**, 2233.

Table 1. Details of Data Collection and Structure Refinement for Complex **1**

compd	**1**
empirical formula	C$_{15}$H$_6$AgAuF$_{10}$O
formula weight	697.03
space group	*C2/c*
V (Å^3)	3546.5(13)
Z	8
D_{calc} (Mg m^{-3})	2.611
a (Å)	20.154(4)
b (Å)	12.091(2)
c (Å)	15.202(4)
β (deg)	106.79(2)
T (K)	173
μ(Mo Kα) (mm^{-1})	9.470
R^a (F, $F > 4\sigma(F)$)	0.0352
wR^b (F^2, all refl.)	0.0885

$^a R(F) = \sum||F_o| - |F_c||/\sum|F_o|.$ $^b wR(F^2) = [\sum\{w(F_o^2 - F_c^2)^2\}/\sum\{w(F_o^2)^2\}]^{0.5}.$

Table 2. Selected Bond Lengths (Å) and Angles (deg) for Complex **1**^{a}

Au−C(11)	2.086(8)	Ag−O(1)	2.353(7)
Au−C(1)	2.092(7)	Ag−C(1)	2.440(8)
Au−Ag#1	2.7829(9)	Ag−C(11)#1	2.506(8)
Au−Ag	2.7903(9)	Ag−Ag#1	3.1810(13)
Au−Au#2	3.1674(11)		
C(11)−Au−C(1)	177.3(3)	Ag#1−Au−Au#2	143.909(18)
C(11)−Au−Ag#1	59.9(2)	Ag−Au−Au#2	137.33(2)
C(1)−Au−Ag#1	121.2(2)	O(1)−Ag−C(1)	101.6(3)
C(11)−Au−Ag	121.8(2)	O(1)−Ag−C(11)#1	94.4(3)
C(1)−Au−Ag	57.9(2)	O(1)−Ag−Au	119.54(18)
Ag#1−Au−Ag	69.61(3)	C(1)−Ag−Au	46.56(16)
C(11)−Au−Au#2	100.9(2)	Au−Ag−Ag#1	55.09(2)
C(1)−Au−Au#2	79.5(2)	Au−C(1)−Ag	75.6(2)

^{a} Symmetry transformations used to generate equivalent atoms: #1, $-x + 1$, $-y + 1$, $-z$; #2, $-x + 1$, y, $-z + \frac{1}{2}$.

Emission lifetimes measurements were performed with an Oriel 79110 N$_2$ laser system (pulse energy 500 ± 20% μJ, pulse output 337.5 nm, 5 ns). The emission signals were detected by a Hamamatsu R1398 photomultiplier tube and recorded on a Tektronix model TDS-250 digital oscilloscope. Error limits are estimated: λ (±0.1 nm); τ (±7%).

Syntheses. Compound **1** was prepared as described by Usón et al.[21b] We have succeeded in obtaining suitable crystals for X-ray diffraction studies by slow diffusion of hexane into a concentrated solution of complex **1** in acetone.

Crystallography. The crystal was mounted in inert oil on a glass fiber and transferred to the cold gas stream of a Siemens P4 diffractometer equipped with an Oxford Instruments low-temperature attachment. Data were collected using monochromated Mo Kα radiation (λ = 0.71073 Å). Scan type $\theta-2\theta$. Cell constants were refined from setting angles of ca. 60 reflections in the 2θ range 10−25°. An absorption correction was applied on the basis of Ψ-scans. The structure was solved by direct methods and refined on F^2 using the program SHELXL-97.[23] All non-hydrogen atoms were refined anisotropically. Hydrogen atoms were included using a riding model. Further details of the data collection are given in Table 1. Selected bond lengths and angles are collected in Table 2.

Computational Methods. The molecular structures used in the theoretical studies of [AuAg(C$_6$H$_5$)$_2$]$_2$ and [AuAg(C$_6$H$_5$)$_2$]$_4$ were taken from the X-ray diffraction results for [AuAg(C$_6$F$_5$)$_2$(OCMe$_2$)]$_n$. Keeping all distances, angles, and dihedral angles frozen, single-point DFT calculations were performed on the models. In both the single-point ground-state calculations and the subsequent calculations of the electronic excitation spectra, the default Beck−Perdew (B−P) functional[24−26] as implemented in TURBOMOLE[27] was employed. The

(23) Sheldrick, G. M. SHELXL-97, A program for crystal structure refinement; University of Göttingen: Göttingen, Germany, 1997.

(24) Vosko, S. H.; Wilk, L.; Nusair, M. *Can. J. Phys.* **1980**, *58*, 1200.
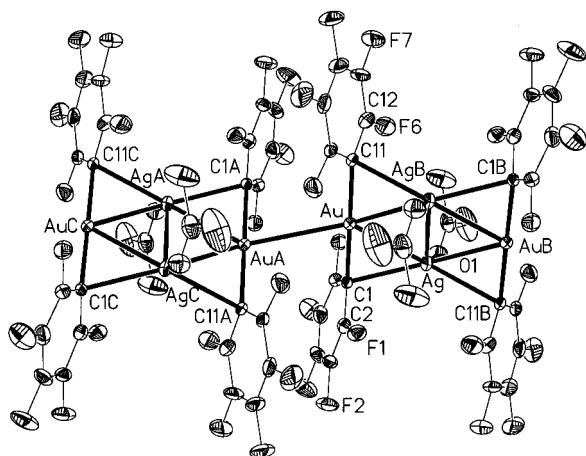
Figure 1. Part of the polymeric chain in complex **1**. Displacement ellipsoids represent 30% probability surfaces. H atoms are omitted for clarity.

excitation energies were obtained at the density functional level using the time-dependent perturbation theory approach (TD-DFT),[28−32] which is a density-functional-theory generalization of the Hartree−Fock linear response (HF-LR) or random phase approximation (RPA) method.[33]

In all calculations, the Karlsruhe split-valence quality basis sets[34] augmented with polarization functions[35] were employed (SVP). The Stuttgart effective core potentials in TURBOMOLE were used for Au and Ag.[36] Calculations were performed assuming C_i symmetry for the monomer and C_2 symmetry for the dimer.

Results and Discussion

Crystal Structure Determination. The structure of complex **1** has been established by an X-ray diffraction study. The compound forms polymeric chains by repetition of the Au_2Ag_2 core, through short Au···Au contacts of 3.1674(11) Å (in Figure 1 two of these units are shown). The molecule lies on a 2-fold symmetry axis, so only half of a molecule resides in the asymmetric unit. Moreover, the Au_2Ag_2 units are repeated by centers of symmetry, thus forming the infinite chain of metal atoms. The silver atoms in the main unit are bonded to two gold atoms with Au−Ag distances of 2.7903(9) and 2.7829(9) Å, which are very similar to those observed in other [(AuAgR₂L)ₙ] complexes (L = tetrahydrothiophene or benzene).[21b] However, there are some differences in the overall bonding scheme in comparison with these latter complexes. First, the two silver centers make a close contact, 3.1810(13) Å, which can be considered a weak bonding interaction. Second, the pentafluorophenyl groups bridge the gold and silver atoms asymmetrically with Au−C distances of 2.086(8) and 2.092(7) Å, which are normal values for pentafluorophenyl gold derivatives, and Ag−C distances of 2.440(8) and 2.506(8) Å. These Ag−C distances are longer than those found in the two crystallographic
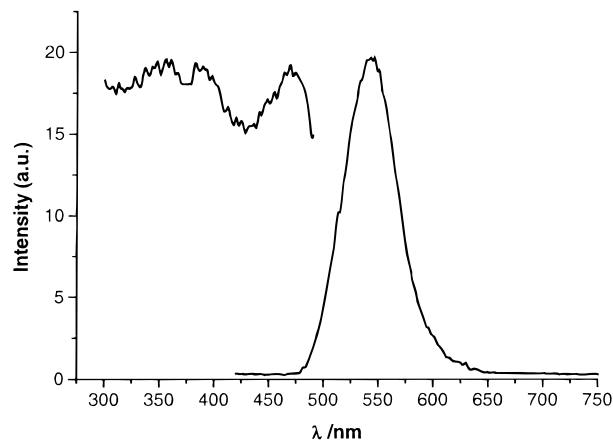
Figure 2. Excitation and emission spectra of compound **1** at room temperature in the solid state.

modifications of the complex [Ag(C₆F₅)(CH₂PPh₃)] (2.105(6) and 2.102(6) Å),[37] and slightly longer than those found in mesityl-bridged silver derivatives such as [Au₂Ag₂(μ-mes)₂(μ-tht)₂(PPh₃)₂] (2.326(3) Å)[38] or [{Au(μ-mes)AsPh₃}₂Ag]ClO₄ (2.27(2) Å),[39] but are similar to those found in the complex [{AuAgR₂(C₆H₆)}ₙ]²¹ᵇ in which the benzene ring is η^2-coordinated to the silver center with Ag−C distances of 2.48 and 2.50 Å. Furthermore, each silver center in complex **1** is also bound to the oxygen atom of the acetone ligand with an Ag−O distance of 2.537(7) Å.

Photophysical Studies. Complex **1** luminesces both at room temperature (see Figure 2) and at 77 K in the solid state. The spectra show a very complicated excitation profile, with a maximum located at 468 nm that leads to a maximum emission band appearing at 546 nm at room temperature which is shifted to 554 nm when the temperature is lowered to 77 K. The reverse trend, i.e. substantial dependence of the emission maxima on the environmental rigidity, which blue shifts the emission band with decreasing temperature, has been reported for some other luminescent complexes[20,40] and has been described as "luminescence rigidochromism".

Lifetime measurements on the microsecond time scale carried out on the standard LS-50B Perkin-Elmer spectrophotometer were beyond the detector capabilities (<10 μs). More accurate time-resolved emission measurements at room temperature reveal that the emissions of solid [Au₂Ag₂(C₆F₅)₄(Me₂CO)₂]ₙ exhibit biexponential decays, showing lifetimes on the nanosecond time scale (τ_1 = 68(5) ns, τ_2 = 298(19) ns; standard deviations are given in parentheses). Similar biexponential decay and lifetime values have been reported by Eisenberg[10] for the complex [Au(S₂CN(C₅H₁₁)₂)]₂ (τ_1 = 60−100 ns, τ_2 = 260−400 ns). The lifetime values, together with the small Stokes shift (ca. 3000 cm⁻¹), suggest that the emission is fluorescence.

This emission is believed to originate from a gold-centered spin-allowed transition (see Calculations section) with an emission wavelength in accord with others previously described.[11] In addition, the blue shift observed in the emission band with increasing temperature is consistent with an increase in the gold−gold separation as a result of thermal expansion. This fact seems to indicate that the gold−gold distance has a

(25) Perdew, J. P. *Phys. Rev. B* **1986**, *33*, 8822.
(26) Becke, A. D. *Phys. Rev. B* **1988**, *38*, 3098.
(27) Ahlrichs, R.; Bär, M.; Häser, M.; Horn, H.; Kölmel, C. *Chem. Phys. Lett.* **1989**, *162*, 165.
(28) Bauernschmitt, R.; Ahlrichs, R. *Chem. Phys. Lett.* **1996**, *256*, 454.
(29) Bauernschmitt, R.; Ahlrichs, R. *J. Chem. Phys.* **1996**, *104*, 9047.
(30) Bauernschmitt, R.; Häser, M.; Treutler, O.; Ahlrichs, R. *Chem. Phys. Lett.* **1997**, *264*, 573 and references therein.
(31) Gross, E. K. U.; Kohn, W. *Adv. Quantum Chem.* **1990**, *21*, 255.
(32) Casida, M. E. In *Recent advances in density functional methods*; Chong, D. P., Ed.; World Scientific: 1995; Vol. 1.
(33) Olsen, J.; Jørgensen, P. In *Modern electronic structure theory*, Vol 2; Yarkony, D. R., Ed.; World Scientific: River Edge, NJ, 1995.
(34) Schäfer, A.; Horn, H.; Ahlrichs, R. *J. Chem. Phys.* **1992**, *97*, 2571.
(35) Dunning, T. H., Jr. *J. Chem. Phys.* **1994**, *100*, 5829.
(36) Andrae, D.; Haeussermann, U.; Dolg, M.; Stoll, H.; Preuss, H. *Theor. Chim. Acta* **1990**, *77*, 123.

(37) Usón, R.; Laguna, A.; Laguna, M.; Usón, A.; Jones, P. G.; Meyer-Bäse, K. *J. Chem. Soc., Dalton Trans.* **1988**, 341.
(38) Contel, M.; Jiménez, J.; Jones, P. G.; Laguna, A.; Laguna, M. *J. Chem. Soc., Dalton Trans.* **1994**, 2515.
(39) Contel, M.; Garrido, J.; Gimeno, M. C.; Jones, P. G.; Laguna, A.; Laguna, M. *Organometallics* **1996**, *15*, 4939.
(40) Lees, A. J. *Chem. Rev.* **1987**, *87*, 711.
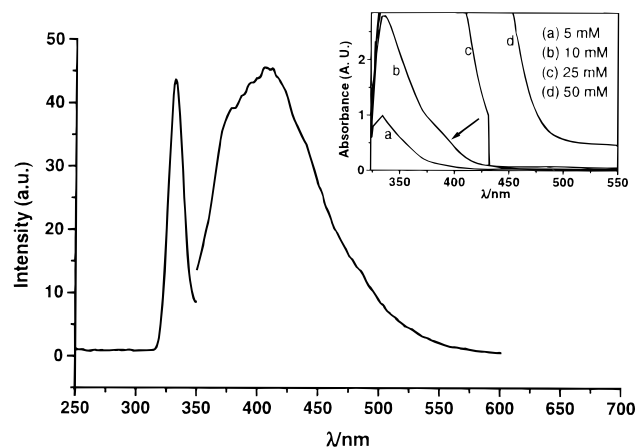
Figure 3. Excitation end emission spectra of **1** in acetone solution $(5 \times 10^{-4}$ M). Inset: Electronic absorption spectra of **1** at different concentrations. The arrow shows the presence of a shoulder.

significant influence on the HOMO-LUMO gap, which increases with increasing Au−Au separation. In fact, as previously reported, the effect of gold−gold interactions roughly produces a destabilization of the $5d_{z^2}$ orbital (with the z axis along the direction of the metal−metal interaction), while the empty $6p_z$ orbital is stabilized. The excitation of an electron from antibonding d to bonding p orbitals yields a net enhancement of intermetallic bonding in the excited state. Although the metal−metal stretching frequency may change, no vibrational fine structure due to such a stretch was observed at 77 or 300 K.

Neither the gold(I) nor the silver(I) precursor complexes are luminescent at similar energies, confirming that the emission is a result of interactions between the metal centers (see calculations).

On the other hand, when the product is dissolved in acetone, the yellow-greenish color of the solid disappears and the resultant colorless solution shows a distinct optical behavior. Thus, a dilute solution $(5 \times 10^{-4}$ M) shows an excitation peak located at 332 nm and an emission at 405 nm (see Figure 3). It is likely that the emission feature arises from pentafluorophenyl-localized $\pi\pi^*$ excited states. Similar phenomena have been analyzed in detail for gold complexes with aromatic substituents.[41] Nevertheless, π-MMCT transitions cannot be excluded (see Calculations section). Evaporation of the solvent regenerates the color and the optical properties. These facts seem to indicate that in a dilute solution the gold−gold interactions are lost. Taking into account the repeat unit in the crystal structure and our calculations (see below), we assume that the resulting species is the unit $[Au_2Ag_2R_4(OCMe_2)_2]$ whose orbital structure does not give an emission as a result of the interactions among the metals; rather, it is mostly the aromatic rings that are involved. One very interesting feature of this complex is that changes in the concentration of the solution give rise to changes in the excitation and emission wavelengths and, therefore, a deviation from Lambert−Beer behavior. Thus, an increase of concentration from 5×10^{-4} to 1.7×10^{-2} M produces the displacement of the excitation and emission bands to 444 and 506 nm, respectively. This tendency is repeated with a further increase in concentration (see Figure 4). In each spectrum the excitation and emission are virtually each other's mirror images with only a small separation between excitation and emission peaks (ca. 50 nm), suggesting that the emission is fluorescence. The absorption spectra of compound **1** in acetone at different

(41) Larson, L. J.; McMacauley, E. M.; Weissbart, B.; Tinti, D. J. *J. Phys. Chem.* **1995**, *99*, 7218.
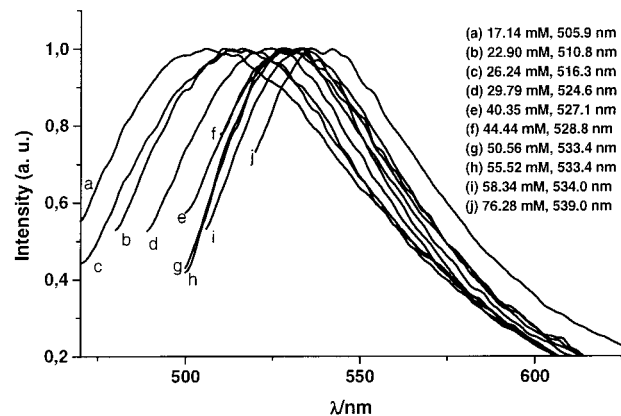
Figure 4. Emission spectra of **1** in acetone solution at different concentrations (see inset). The intensities of all curves are normalized.

concentrations have a common band whose maximum is located at 334 nm, in accord with the excitation observed in dilute solutions. Similar behavior has been found by Lin and co-workers[18a] for aromatic phenyl groups. Careful examination of the spectra from 5×10^{-3} M up to higher concentrations shows that the intensity of the band arising from the ligands is concentration dependent while the shoulder that appears near 400 nm does not obey Lambert−Beer's law and appears at lower energy when the concentration increases (see inset in Figure 3).

This deviation from Lambert−Beer's law is consistent with molecular aggregation in fluid solution. In fact, the red shift observed when the concentration increases is in agreement with the correlation between the nuclearity enhancement and the metal-centered transition energy,[42] because as the number of Au−Au interactions increases, the HOMO-LUMO gap is reduced. Gray and co-workers reported $[Pt(tpy)Cl]^+$ to undergo oligomerization in solution to yield low-energy visible absorption at 400−550 nm.[43,44] Concentration-dependent emission spectra in gold(I) or platinum(II) compounds were reported as evidence for molecular association,[10,17−20] but to the best of our knowledge, no study has previously shown a clear correlation between the emission wavelength and the structure in solution and in the solid state.

If we represent the emission wavelength (y axis) versus the inverse of the concentration (x axis), we observe linear behavior (see Figure 5). Here we can assume that the zero value on the x axis represents the situation in the solid state because there the concentration can be considered infinite. Indeed, the extrapolated value obtained, which is given in the linear fit equation $y = -0.75x + 547.04$ when x is equal to zero, perfectly matches the emission value in the solid state (experimental 546.0 nm, obtained 547.04 nm). Thus, we can conclude that the different wavelength values at different concentrations arise from aggregation of $[Au_2Ag_2(C_6F_5)_4(OCMe_2)_2]$ units through gold−gold interactions.

Ground-State DFT Calculations. In light of the results reported in the spectroscopic section, single-point DFT calculations have been performed with two different models: the $[Au_2Ag_2(C_6H_5)_4]$ or "monomer" model, which represents the molecule in solution at low concentrations $(5 \times 10^{-4}$ M), and the $[Au_2Ag_2(C_6H_5)_4]_2$ or "dimer" model as an approximation

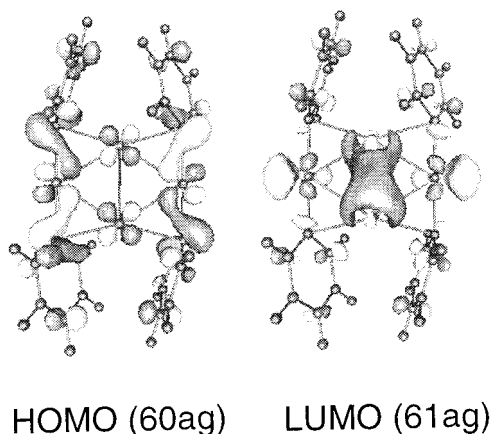(42) Yam, V. W.-W.; Lai, T.-F.; Che, C.-M. *J. Chem. Soc., Dalton Trans.* **1990**, 3747.

(43) Bailey, J. A.; Hill, M. G.; Marsh, R. E.; Miskowski, V. M.; Schaefer, W. P.; Gray, H. B. *Inorg. Chem.* **1995**, *34*, 4591.

(44) Hill, M. G.; Bailey, J. A.; Miskowski, V. M.; Gray, H. B. *Inorg Chem.* **1996**, *35*, 4585.
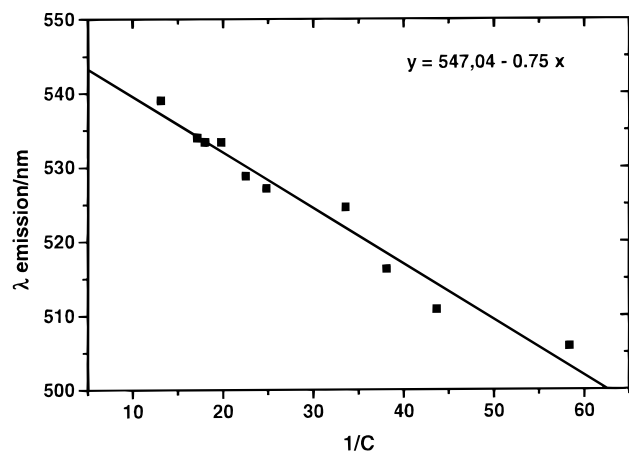
Figure 5. Representation of the inverse of the concentration (1/C) vs the emission wavelength (λ emission/nm). The intercept is 547.04 $\pm$ 1.65 nm.

HOMO (60ag)   LUMO (61ag)

Figure 6. HOMO and LUMO molecular orbitals for the [AuAg-$(C_6H_5)_2]_2$ model system.

Table 3. Population Analysis for the $[Au_2Ag_2(C_6H_5)_4]$ Model System; Contribution from Each Type of Atom to Occupied Orbitals

MO	% Au	% Ag	% C	% H
HOMO (60ag)	15.31	11.41	70.87	2.4
HOMO−1 (60au)	18.13	8.86	68.28	4.73
HOMO−2 (59au)	38.27	17.66	41.72	2.33
HOMO−3 (59ag)	9.15	4.52	81.41	4.92
HOMO−4 (58ag)	5.27	12.56	82.17	
HOMO−5 (58au)	8.29	5.56	86.05	0.1
HOMO−6 (57au)	13.08	13.08	73.04	0.8
HOMO−7 (56au)	9.5	15.37	75.02	0.1
HOMO−9 (56ag)	36.25	4.63	57.9	1.21
HOMO−10 (55au)	18.91	7.24	73.44	0.4

Table 4. Population Analysis for the $[Au_2Ag_2(C_6H_5)_4]_2$ Model System; Contribution from Each Type of Atom to Occupied Orbitals

MO	% Au	% Ag	% C	% H
HOMO (120b)	51.3	15.67	32.87	0.15
HOMO−1 (120a)	13.58	11.73	72.53	2.16
HOMO−2 (119b)	16.31	11.82	70.03	1.83
HOMO−3 (119a)	9.26	7.55	77.74	5.44
HOMO−4 (118b)	8.46	8.86	77.04	5.64
HOMO−5 (118a)	43.26	18.57	37.34	0.82
HOMO−6 (117b)	11.08	4.88	79.17	4.88
HOMO−8 (116b)	19.47	12.74	67.79	
HOMO−11 (115b)	9.13	5.78	85.09	
HOMO−13 (114b)	11.51	12.52	75.36	0.6
HOMO−15 (112b)	12.41	15.06	72.43	0.1

HOMO (120b)   LUMO (121a)
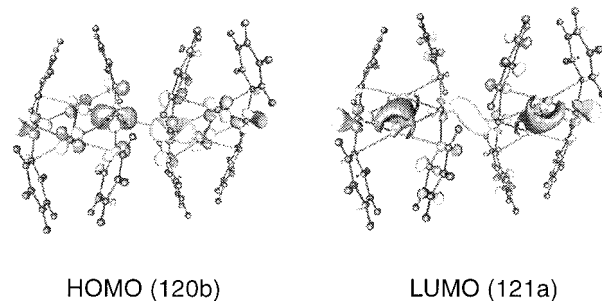
Figure 7. HOMO and LUMO molecular orbitals for the [AuAg-$(C_6H_5)_2]_4$ model system. Notice the 5d antibonding character of the HOMO and the 6p bonding character of the LUMO, between the Au atoms.

to the structure of the molecule in the solid state. Both the "monomer" and the "dimer" models have been built from the X-ray diffraction results for complex **1**.

Regarding the "monomer" model, we have performed a study of its MO's and a population analysis to check the contribution of each atom to each occupied orbital. The HOMO and LUMO are given in Figure 6. The results are given in Table 3 and the analysis of these data shows that from HOMO to HOMO−10 the main important contribution to the orbitals comes from the C atoms; therefore, the highest occupied orbitals in this model are proposed to be localized on the aromatic rings. On the other hand, the lowest unoccupied orbitals (from LUMO to LUMO+5) cannot be analyzed by a population analysis but we can check the shape of these orbitals. LUMO and LUMO+1 are localized both on the metals and on the ligands, but mainly on silver. Notice the shape of the LUMO in Figure 6: it corresponds mostly to the $5p_z$ Ag−Ag bonding MO, while the orbitals from LUMO+2 to LUMO+5 are localized on the ligands. So we can predict that in solution we would observe an excitation profile due to transitions arising from the ligands.

The next step was the same calculation as before but on the dimer model. In this case the population analysis (see Table 4) shows, in general, the same behavior as in the monomer: orbitals from HOMO−1 to HOMO−10 are mainly localized on the ligands. The only difference arising from the introduction of the gold−gold interaction is observed in the HOMO orbital. For this orbital, the population analysis shows that the HOMO

is mainly localized on the gold atoms. Also the shape of the orbital in the region near the gold atoms involved in an intermolecular interaction reveals a clear $nd_{z^2}\sigma^*$ character that is in accord with the proposed character of the HOMO in gold dimers when a gold−gold interaction is present (Figure 7). Another interesting feature is observed in the LUMO, in which we find bonding electronic density between the two gold atoms that are in close contact (see Figure 7). This is, again, in accord with the previously described character of the LUMO for the $[Au_2(P−P)_2]^{2+}$ case in which a Au−Au intramolecular interaction is found and $np\sigma$ character is assumed.[15] For the next unoccupied orbitals we observe that LUMO+1 is localized both on metals and ligands and LUMO+2 and LUMO+3 are localized mainly on the Ag atoms.

TD-DFT Calculations. The first few singlet excitation energies of the $[Au_2Ag_2(C_6H_5)_4]$ and $[Au_2Ag_2(C_6H_5)_4]_2$ model systems were calculated at the TD-DFT level as described in the computational methods section. We cannot presently estimate the strength, given by spin−orbit effects to the triplet transitions. Only singlet−singlet transitions were considered in

Table 5. TD-DFT RPA Singlet-Excitation Calculations for [$Au_2Ag_2(C_6H_5)_4$]

| excitation	λ_{calc} (nm)	λ_{exp} (nm)	oscil. str.[a] (s)	contributions[b]
A	411.9		0.273×10^{-1}	$60ag \rightarrow 61au$ (66.7)
				$59au \rightarrow 61ag$ (26.1)
B	398.4		0.234×10^{-1}	$59au \rightarrow 61ag$ (51.3)
				$60ag \rightarrow 61au$ (32.6)
				$60au \rightarrow 61ag$ (8.3)
C	364.5		0.138×10^{-1}	$58au \rightarrow 61ag$ (88.9)
				$56au \rightarrow 61ag$ (4.1)
D	356		0.577×10^{-1}	$57au \rightarrow 61ag$ (86.4)
				$56au \rightarrow 61ag$ (8.2)
E	346.3		0.591×10^{-1}	$56au \rightarrow 61ag$ (78.2)
				$57au \rightarrow 61ag$ (6.2)
				$59ag \rightarrow 61au$ (5.7)
F	333.5	333	0.160×10^{-1}	$59ag \rightarrow 61au$ (92.6)
G	322.6		0.631×10^{-1}	$55au \rightarrow 61ag$ (87.4)
				$60ag \rightarrow 62au$ (4.1)
H	316.8		0.442×10^{-1}	$60ag \rightarrow 62au$ (44.1)
				$58ag \rightarrow 61au$ (43.2)
				$60au \rightarrow 62ag$ (3.0)
I	314		0.389×10^{-1}	$58ag \rightarrow 61au$ (51.5)
				$60ag \rightarrow 62au$ (27.8)
				$60au \rightarrow 62ag$ (11.2)
J	310.9		0.150×10^{-1}	$60au \rightarrow 62ag$ (81.8)
				$60ag \rightarrow 62au$ (9.7)

[a] Oscillator strength shows the mixed representation of both velocity and length representations. [b] Value is $|coeff.|^2 \times 100$.

these, quasirelativistic calculations. No experimental singlet−triplet assignments were presented.

[$Au_2Ag_2(C_6H_5)_4$] Model System. For an idealized structure of compound **1** at low concentrations with a tetranuclear [$Au_2Ag_2(C_6H_5)_4$] model, symmetry labels corresponding to the C_i point group can be used. In this case the symmetry of the excited state is a_u. In Table 5, the first 10 transition energies for this model system are compared to the experimental excitation energies in solution at low concentration (5×10^{-4} M). In Figure 8 we can observe that the theoretical excitations labeled A and B do not match the experimental excitation spectra, but they match the experimental absorption spectra. That means that excitations A and B do not give rise to emission of radiation. On the other hand from excitation C to J we find very good agreement, for both the energy and the relative oscillator strength, with the experimental excitation spectra. For these excitations the calculation gives the MO's involved in each transition (see Table 5). The subsequent analysis of the character of these orbitals shows that from C to J all the excitations come from orbitals mainly localized on the ligands ($60a_g$, $59a_u$, $60a_u$, $58a_u$, $57a_u$, $56a_u$, and $55a_u$, see Table 3) to orbitals mainly localized on the silver atoms. Thus, we can conclude that the emission of compound **1** in solution at low concentration is due to a transition arising from the ligands to π^* orbitals of the ligands or metal based bonding orbitals. This fact could explain the emission profile obtained under these conditions, because its maximum appears at 405 nm, which is the region in which aromatic ligand transitions appear.[41]

[$Au_2Ag_2(C_6H_5)_4$]$_2$ Model System. In this case we assume that the introduction of one gold−gold interaction that links two "monomer" units could represent, as a theoretical model, the solid-state situation for compound **1**. This new arrangement produces a change in the symmetry, which goes from point group C_i in the "monomer" model system to C_2 in the "dimer" model system in which b is now the symmetry of the excited state. By checking Laporte's rule we observe that for the point group C_2 the HOMO-LUMO transition is dipole-allowed in
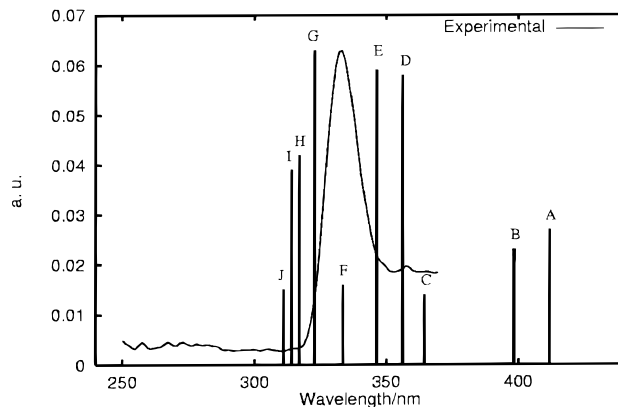
Figure 8. Experimental excitation spectrum for complex **1** at the concentration 5×10^{-4} M in arbitrary units and theoretical oscillator strengths, *f*, from Table 4 for the monomer model [$Au_2Ag_2(C_6H_5)_4$].
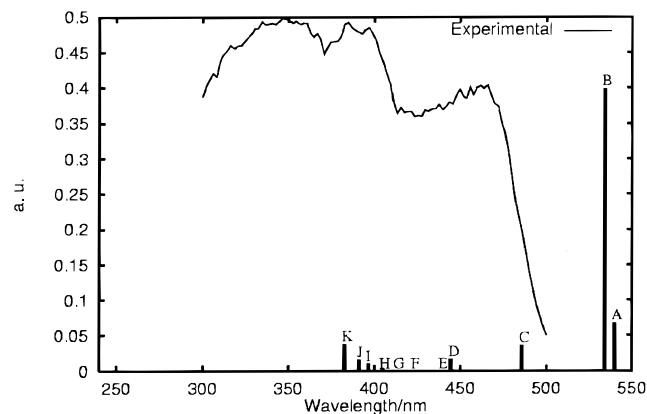
Figure 9. Experimental excitation spectrum for complex **1** in the solid state in arbitrary units and theoretical oscillator strengths, *f*, from Table 5 for the dimer model [$Au_2Ag_2(C_6H_5)_4$]$_2$. Note the increase of *f* from Figure 8.

contrast to the monomer model. In Figure 9 the calculated excitations A to K are compared with the experimental excitation spectrum of **1** in the solid state. In this case the predicted energy values for the excitations show differences from those obtained from the experiment, maybe due to the inclusion of only one gold−gold interaction, which does not represent the situation in the solid state. Nevertheless, we can separate both the experimental and the predicted spectra into three equivalent groups of signals (from A to B, from C to E, and from F to K) that show relative energy difference among them with good accord between the experimental and the predicted spectra (see also Table 6). Another interesting aspect of the predicted excitations is their oscillator strength values, which for excitation B are much larger than for the rest. The analysis of this excitation shows that the more important orbitals involved in this transition are 120b or HOMO and 121a or LUMO. This predicted transition at 534 nm can be assigned to the experimental maximum at 465 nm and, therefore, is in accord with the previously assigned[11] $5d_{z^2}\sigma^*-6p\sigma$ transitions due to the aforementioned character of the HOMO (120b) and LUMO (121a) orbitals.

Conclusions

The polynuclear gold−silver compound **1** reported in this paper exhibits luminescence arising from $\pi\pi^*$ excited states in the pentafluorophenyl ligands or from π-MMCT transitions when dilute acetone solutions are measured. In contrast, metal-

Table 6. TD-DFT RPA Singlet-Excitation Calculations for [Au₂Ag₂(C₆H₅)₄]₂

excitation	λ_{calc} (nm)	λ_{exp} (nm)	oscil. str.[a] (s)	contributions[b]
A	539.6		0.677×10^{-1}	119b → 121a (83.3)
				120b → 121a (15.7)
B	533.9	469	0.399^1	120b → 121a (80.3)
				119b → 121a (26.1)
C	485.7	382.5	0.362×10^{-1}	118b → 121a (97.6)
D	444.4		0.175×10^{-1}	120a → 121b (93.4)
E	439.2		0.275×10^{-3}	120b → 122a (93.2)
F	422.7		0.397×10^{-3}	117b → 121a (96.6)
G	412.3		0.357×10^{-3}	120a → 122b (76.6)
				119b → 122a (23.1)
H	404.8		0.399×10^{-2}	119a → 121b (96.1)
I	396.5	355.5	0.106×10^{-1}	116b → 121a (88.8)
				115b → 121a (3.2)
J	391.3		0.164×10^{-1}	115b → 121a (89.2)
				114b → 121a (4.8)
K	382.7		0.376×10^{-1}	114b → 121a (79.6)
				112b → 121a (9.1)
				118b → 122a (3.5)

a Oscillator strength shows the mixed representation of both velocity and length representations. *b* Value is |coeff.|² × 100.

centered $(d\sigma^*)^1(p\sigma)^1$ or $(d\delta^*)^1(p\sigma)^1$ excited states are responsible for the luminescence in the solid state. This class of compound is a luminophore with potentially tunable excited-state properties.

The special structural features of the Au₂Ag₂ unit are appropriate for this study because they act as building-blocks that form polymeric chains. The intermediate self-aggregation ratio obtained when concentration increases can be observed in either the absorption or emission spectrum. The latter allows us to establish a clear correlation between the aggregation process through gold−gold contacts in solution and the emissive behavior in acetone solution and in the solid state by a simple linear fit. Extrapolation to infinite concentration clearly matches the solid-state emission.

This assignment, as well as the previously reported character of the molecular orbitals, is in accord with the TD-DFT calculations performed in this work. Moreover, for the first time, this type of calculation has been used for the explanation of the excitations that lead to emission of radiation in solution and in the solid state.

Supporting Information Available: X-ray crystallographic parameters for compound **1** (PDF). This material is available free of charge via the Internet at http://pubs.acs.org.

JA9942540